



OPEN ACCESS

EDITED BY
Kristin Stanford,
The Ohio State University, United States

REVIEWED BY
David Wright,
University of Guelph, Canada
Emmanuelle Havis,
Sorbonne Universités, France

*CORRESPONDENCE
Roger D. Cox,
roger.cox@adipogenetics.co.uk
Rebecca Dumbell,
rebecca.dumbell@ntu.ac.uk

†These authors share last authorship

SPECIALTY SECTION
This article was submitted to Integrative
Physiology,
a section of the journal
Frontiers in Physiology

RECEIVED 25 May 2022
ACCEPTED 19 July 2022
PUBLISHED 25 August 2022

CITATION
Mušo M, Bentley L, Vizor L, Yon M,
Burling K, Barker P, Zolkiewski LAK,
Cox RD and Dumbell R (2022), A *Wars2*
mutant mouse shows a sex and diet
specific change in fat distribution,
reduced food intake and depot-specific
upregulation of WAT browning.
Front. Physiol. 13:953199.
doi: 10.3389/fphys.2022.953199

COPYRIGHT
© 2022 Mušo, Bentley, Vizor, Yon,
Burling, Barker, Zolkiewski, Cox and
Dumbell. This is an open-access article
distributed under the terms of the
[Creative Commons Attribution License
\(CC BY\)](https://creativecommons.org/licenses/by/4.0/). The use, distribution or
reproduction in other forums is
permitted, provided the original
author(s) and the copyright owner(s) are
credited and that the original
publication in this journal is cited, in
accordance with accepted academic
practice. No use, distribution or
reproduction is permitted which does
not comply with these terms.

A *Wars2* mutant mouse shows a sex and diet specific change in fat distribution, reduced food intake and depot-specific upregulation of WAT browning

Milan Mušo¹, Liz Bentley^{1,2}, Lucie Vizor², Marianne Yon²,
Keith Burling³, Peter Barker³, Louisa A. K. Zolkiewski¹,
Roger D. Cox^{1*†} and Rebecca Dumbell^{1,4*†}

¹Mammalian Genetics Unit, MRC Harwell Institute, Oxfordshire, United Kingdom, ²Mary Lyon Centre at MRC Harwell, Oxfordshire, United Kingdom, ³MRC Metabolic Diseases Unit, Mouse Biochemistry Laboratory, Cambridge, United Kingdom, ⁴Department of Biosciences, School of Science and Technology, Nottingham Trent University, Nottingham, United Kingdom

Background: Increased waist-to-hip ratio (WHR) is associated with increased mortality and risk of type 2 diabetes and cardiovascular disease. The *TBX15-WARS2* locus has consistently been associated with increased WHR. Previous study of the hypomorphic *Wars2*^{V117L/V117L} mouse model found phenotypes including severely reduced fat mass, and white adipose tissue (WAT) browning, suggesting *Wars2* could be a potential modulator of fat distribution and WAT browning.

Methods: To test for differences in browning induction across different adipose depots of *Wars2*^{V117L/V117L} mice, we measured multiple browning markers of a 4-month old chow-fed cohort in subcutaneous and visceral WAT and brown adipose tissue (BAT). To explain previously observed fat mass loss, we also tested for the upregulation of plasma mitokines FGF21 and GDF15 and for differences in food intake in the same cohort. Finally, to test for diet-associated differences in fat distribution, we placed *Wars2*^{V117L/V117L} mice on low-fat or high-fat diet (LFD, HFD) and assessed their body composition by Echo-MRI and compared terminal adipose depot weights at 6 months of age.

Results: The chow-fed *Wars2*^{V117L/V117L} mice showed more changes in WAT browning marker gene expression in the subcutaneous inguinal WAT depot (iWAT) than in the visceral gonadal WAT depot (gWAT). These mice also demonstrated reduced food intake and elevated plasma FGF21 and GDF15, and mRNA from heart and BAT. When exposed to HFD, the *Wars2*^{V117L/V117L} mice showed resistance to diet-induced obesity and a male and HFD-specific reduction of gWAT: iWAT ratio.

Conclusion: Severe reduction of *Wars2* gene function causes a systemic phenotype which leads to upregulation of FGF21 and GDF15, resulting in reduced food intake and depot-specific changes in browning and fat mass.

KEYWORDS

WARS2, WHR, fat distribution, browning, GDF15, FGF21, food intake, waist-hip ratio

Introduction

Increased waist-to-hip ratio (WHR) is associated with increased mortality and risk of coronary heart disease, myocardial infarction and type 2 diabetes (Snijder et al., 2003; Wang et al., 2005; Vazquez et al., 2007; Canoy, 2008; Mason et al., 2008; Myint et al., 2014; Emdin et al., 2017; Peters et al., 2018). The most recent meta-analysis identified 346 different loci associated with WHR adjusted for body mass index (WHRadjBMI) with most of the candidate genes being enriched in adipocytes and multiple fat depots (Pulit et al., 2018).

The *TBX15-WARS2* locus, which spans ~1 Mb and includes genes *TBX15*, *WARS2* and regions downstream of *SPAG17*, is consistently associated with WHR across multiple meta-analyses (Heid et al., 2010; Shungin et al., 2015; Pulit et al., 2018). Since the majority of SNPs in this region overlap the non-coding part of the genome, the effector genes remain to be identified (Maurano et al., 2012; Mušo et al., 2022). *WARS2* is a mitochondrial tryptophanyl-tRNA synthetase, a protein essential for mitochondrial translation, recently associated with angiogenesis and brown adipose tissue metabolism (Wang et al., 2016; Pravenec et al., 2017). Expression of both *TBX15* and *WARS2* in subcutaneous adipose tissue was associated with multiple metabolic traits including BMI and Matsuda insulin sensitivity index (Civelek et al., 2017). The GTEx database links the *TBX15-WARS2* locus risk SNPs to the expression of *WARS2* in multiple human tissues, but a few studies have also linked the locus to *TBX15* expression in adipose (Heid et al., 2010; GTEx-Consortium, 2013; Civelek et al., 2017).

Our group has previously established a *Wars2*^{V117L/V117L} mouse model where a N-ethyl-N-nitrosourea (ENU)-induced hypomorphic mutation causes defective splicing and results in only 0%–30% of the full-length protein remaining across different tissues (Agnew et al., 2018). Homozygous *Wars2*^{V117L/V117L} mice showed mitochondrial electron transport chain (ETC) complex deficiency in multiple tissues which directly or indirectly resulted in hypertrophic cardiomyopathy, sensorineural hearing loss and failure to gain fat mass. Importantly, white adipose tissue (WAT) showed upregulation of mitochondria and browning markers such as uncoupling protein 1 (UCP1) and mRNA levels of cell death-inducing DNA fragmentation factor subunit alpha (DFFA)-like effector a (*Cidea*) and iodothyronine deiodinase 2 (*Dio2*) genes. On the other hand, the brown adipose tissue (BAT) was dysfunctional and showed reduced browning marker expression. Elevated serum fibroblast growth factor-21 (FGF21) and mRNA from heart, muscle and white

adipose suggested a mechanism by which at least part of the browning in adipose tissue may be mediated systemically (Fisher et al., 2012).

Another mitokine frequently co-induced with FGF21 in response to mitochondrial stress is growth/differentiation factor 15 (GDF15). GDF15 was previously reported to be an inducer of taste aversion and a suppressor of food intake by acting in the hindbrain where its receptor GDNF family receptor α -like (GFRAL) is expressed (Mullican et al., 2017; Patel et al., 2019). We hypothesised that a possible elevation of GDF15 levels could be thus affecting food intake and in effect the fat mass in *Wars2*^{V117L/V117L} mice.

In this follow-up study, we set out to explore whether *WARS2* could be a regulator of white adipose browning and fat distribution. We initially tested whether the previously observed WAT browning effects in *Wars2*^{V117L/V117L} mice differed between different depots and whether changes in FGF21, GDF15, and food intake are observed and thus could explain the failure to gain fat mass in the chow-fed mice. Given that human polymorphisms in the *TBX15-WARS2* locus are associated with a less severe reduction in *WARS2* expression (GTEx-Consortium, 2013), we included heterozygous *Wars2*^{+/V117L} mice in our study. We evaluated the effect of high- and low-fat diet challenge (HFD—60% kcal fat, LFD—10% kcal fat) on adiposity and tested for any diet and depot specific differences in fat mass loss.

Materials and methods

Animal models

All mice used in this study were housed in the Mary Lyon Centre at MRC Harwell. Mice were kept and studied in accordance with UK Home Office legislation and local ethical guidelines issued by the Medical Research Council (Responsibility in the Use of Animals for Medical Research, July 1993; Home Office license 30/3146 and 30/3070). Procedures were approved by the MRC Harwell Animal Welfare and Ethical Review Board (AWERB). Mice were kept under controlled light (light 7 a.m.–7 p.m., dark 7 p.m.–7 a.m.), temperature (21°C \pm 2°C) and humidity (55% \pm 10%) conditions. They had free access to water (9–13 ppm chlorine) and were fed *ad libitum* on a commercial chow diet (SDS Rat and Mouse No. 3 Breeding diet, RM3, 3.6 kcal/g) unless stated otherwise. Mice were group housed unless stated otherwise and were randomised into sex-matched cages on weaning. Researchers were blinded to the genotype of mice until analysis of the data.

Experiment 1—molecular and hormonal investigation of *Wars2*^{V117L/V117L} mice

Wars2^{V117L/V117L} mice were generated and genotyped as previously described (Potter et al., 2016; Agnew et al., 2018). Tissues and plasma were collected in experiments previously described (Agnew et al., 2018). Briefly, 4-month-old male and female *Wars2*^{V117L/V117L} and *Wars2*^{+/+} mice ($n = 5-7$) were humanely killed by terminal anaesthesia, and retro-orbital blood was collected into lithium-heparin microvette tubes (CB300, Sarstedt, Numbrecht, Germany). Death was confirmed by cervical dislocation and mice were then dissected and kidney, liver, muscle, heart, iWAT, gWAT, and BAT collected. Tissues were directly placed in cryotubes and snap frozen in liquid nitrogen and samples were stored at -70°C before subsequent analyses by qPCR and Western blot.

Experiment 2—food intake measurements in *Wars2*^{V117L/V117L} mice

Four-week-old male and female *Wars2*^{V117L/V117L}, *Wars2*^{+/V117L}, and *Wars2*^{+/+} mice were pair-housed by genotype with *ad libitum* access to RM3 diet ($n = 4-10$ cages). Food was weighed twice a week until 16 weeks of age, and mice were weighed weekly. The mean weekly food intake per week per cage was calculated and cumulative food intake analysed.

Experiment 3—body fat distribution in *Wars2*^{V117L/V117L} mice on HFD

We investigated body composition and fat distribution in male and female *Wars2*^{V117L/V117L}, *Wars2*^{+/V117L}, and *Wars2*^{+/+} mice challenged with a high-fat diet (HFD). Experimental cohort numbers were based on estimates made using GraphPad Statmate using gWAT:iWAT ratios from previous experiments. We generated three cohorts of males and females, which were weaned directly onto HFD (*Research Diets*, D12492) or matched low-fat diet (LFD, *Research Diets*, D12450) ($n = 9-22$, 185 mice in total).

Total body mass was measured every 2 weeks from 4 weeks of age on a scale calibrated to 0.01 g. Body composition of the mice was measured every 2 weeks using an Echo-MRI (EMR-136-M, Echo-MRI, Texas, United States). The readings were total fat mass (g) and total lean mass (g). At 24 weeks old, mice were humanely killed by cervical dislocation and individual fat depots were dissected and weighed: interscapular BAT (iBAT), interscapular WAT (isWAT), perirenal BAT (prBAT), perirenal WAT (prWAT), inguinal WAT (iWAT), gonadal WAT (gWAT), mesenteric WAT (mWAT), and epicardial WAT (cWAT). gWAT:iWAT ratio was calculated from these

weights as an indicator of visceral:subcutaneous fat distribution as described in (Gray et al., 2006).

Experiment 4—body weight and composition in heterozygous knockout *Wars2*^{+/-} mice on HFD

NIH KOMP *Wars2*^{+/-} mice (*Wars2*^{tm1(KOMP)Vlsg}) obtained from the KOMP repository (<https://www.komp.org/>) were imported into our laboratory previously (Agnew et al., 2018). Female *Wars2*^{+/-} and *Wars2*^{+/+} mice were weaned directly onto HFD or LFD ($n = 7-9$, 32 mice) and maintained until 12 months when they were weighed, and body composition analysed by Echo-MRI (EMR-136-M, Echo-MRI, Texas, United States). At 12 months old, mice were humanely killed by cervical dislocation and individual fat depots were dissected and weighed as in experiment 3.

Quantitative PCR

Total RNA from adipose tissues (experiment 1) was extracted using the Direct-zol™ RNA MiniPrep Plus kit protocol (Zymo research, #R2071). RNA was reverse-transcribed using the SuperScript™ III Reverse Transcriptase Kit (ThermoFisher) to generate 2 μg of cDNA. mRNA gene expression was assayed using the TaqMan system (ThermoFisher) with the TaqMan FAM dye-labeled probes (Applied Biosystems, Invitrogen, United States) according to manufacturer protocols. Assays were carried out using an ABI PRISM 7500 Fast Real-Time PCR System (Applied Biosystems) and quantitation by the comparative C_T ($\Delta\Delta\text{C}_T$) analysis. Data was normalised to a geometric mean of two house-keeping genes specific to each tissue.

A mouse GeNORM analysis (PrimerDesign) for 6–8 genes was used to determine the most stable house-keeping genes. Taqman probes used in this study: *Canx* (Mm00500330_m1), *Rpl13a* (Mm01612986_gH), *Wars2* (Mm04208965_m1), *Ywhaz* (Mm01722325_m1), *Cidea* (Mm0042554_m1), *Cox7a1* (Mm00438297_g1), *Dio2* (Mm00515664_m1), *Ucp1* (Mm01244861_m1), *Fgf21* (Mm00840165_g1), *β-klotho* (Mm00502002_m1), *Pgc1α* (Mm01208835_m1), *Ppara* (Mm00440939_m1), *Ppary* (Mm01184322_m1), *Prdm16* (Mm00712556_m1).

Immunoblotting

Tissues were homogenised in CelLytic MT Mammalian Tissue Extraction Reagent (Sigma) supplemented with cOMplete Protease Inhibitor (Sigma) and PhosSTOP Inhibitor (Sigma) using the Precellys-24 automated homogeniser (Bertin

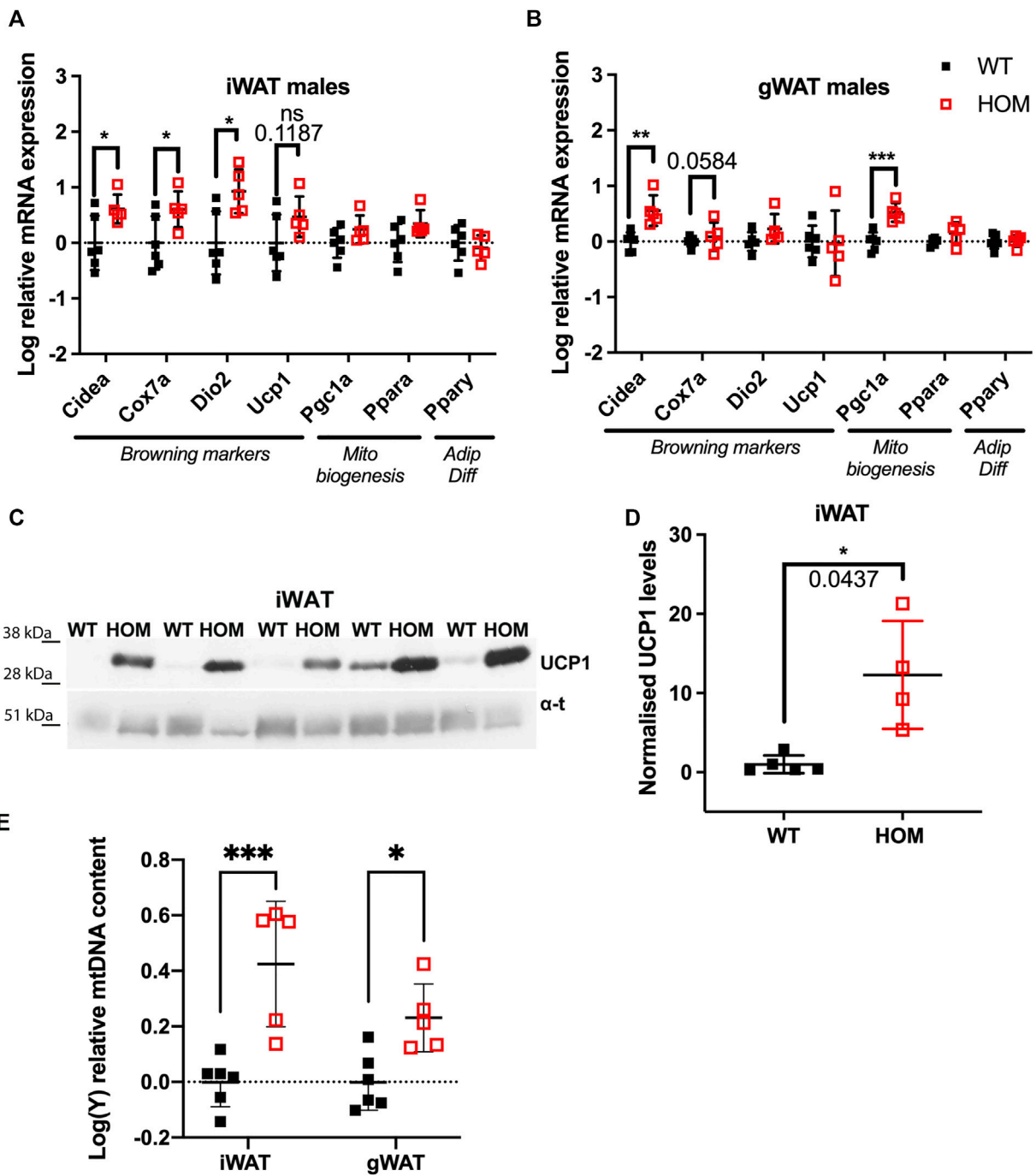
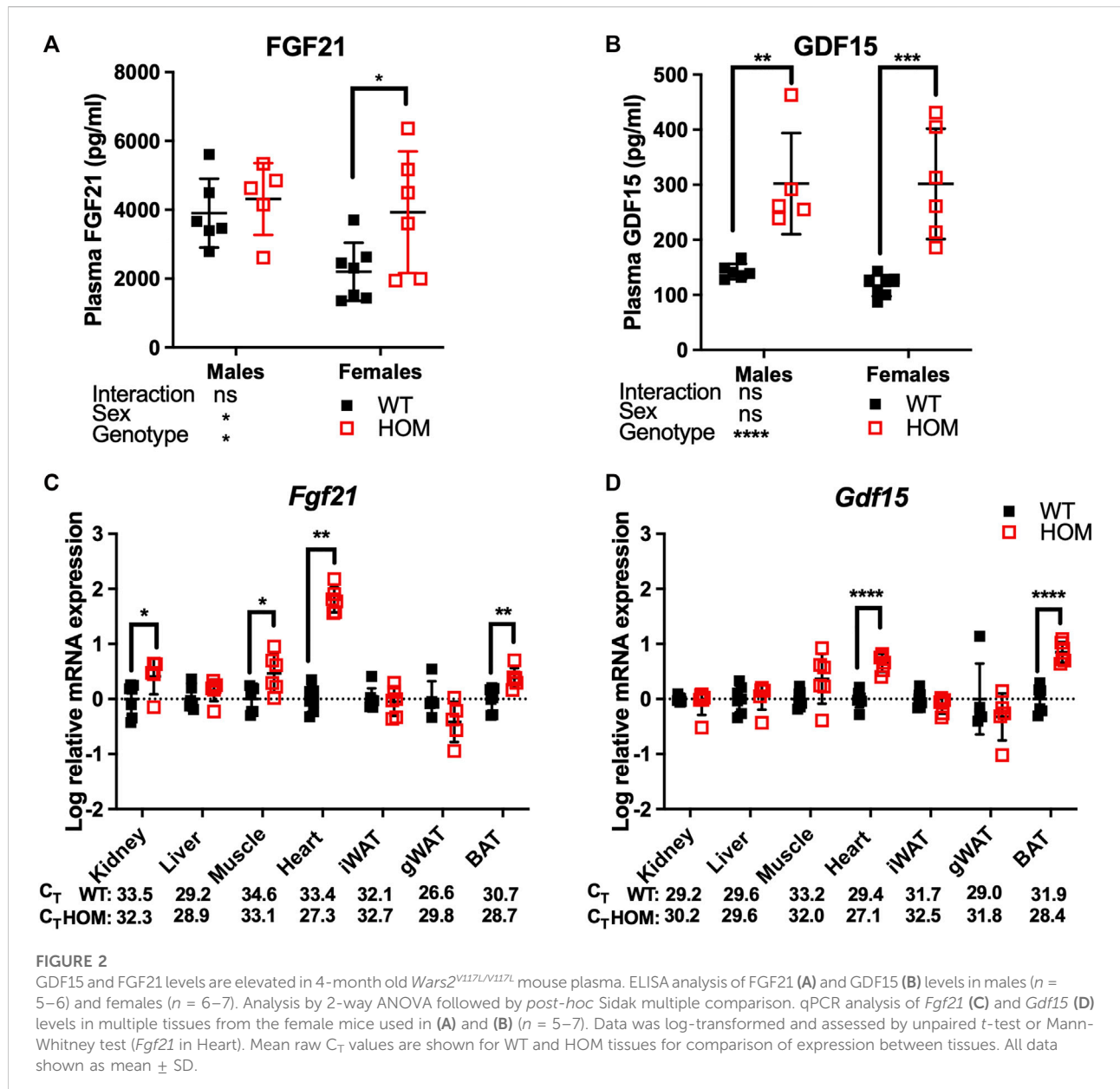


FIGURE 1
 Increased browning in inguinal WAT (iWAT) and gonadal WAT (gWAT) of 4-month old male *Wars2^{V117L/V117L}* mice. (A,B) Relative expression of browning, mitochondrial biogenesis and adipose differentiation markers in iWAT and gWAT, respectively. Normalised to geometric mean of *Canx* and *Ywhaz*. Data was log-transformed and assessed by unpaired *t*-test or Mann-Whitney test (iWAT for *Dio2* and *Fgf21*) based on their distribution, *n* = 6 and five wildtype and homozygotes respectively in iWAT and gWAT. (C,D) Western blot and quantification of UCP1 protein levels in male iWAT relative to α -tubulin and WT average, *n* = 5. Tested by Unpaired *t* test with Welch's correction (E) qPCR analysis of *mt-Nd1:Gapdh* ratio signifying mitochondrial: genomic DNA (mtDNA:gDNA) ratio. 2-way ANOVA with *post-hoc* comparison of genotypes, *n* = 5. All data shown as mean \pm SD.



Instruments). Tissue homogenates were centrifuged at 13,000 rpm for 30 min at 4°C. For adipose samples, the floating lipid layer was carefully pierced with a P200 pipette tip, the supernatant transferred to a new Eppendorf tube and samples spun again 1-2 more times until all lipid was removed. The final supernatants were isolated and protein concentration quantified by the DC Protein Assay (BioRad). The samples were diluted and supplemented with NuPAGE LDS Sample Buffer (4X) and NuPage Reducing Agent (10X) and were denatured by heating to 70°C for 10 min. Gel electrophoresis was performed using the linear gradient NuPAGE 4%–12% Bis-Tris Protein Gels, 1.0 mm, 12-well (ThermoFisher) with 1X NuPAGE MOPS SDS Running Buffer in the Mini Gel Tank (ThermoFisher). 20 µg

protein was loaded per well and samples run at 200 V for 50 min. The experimental and control groups (WT, HOM) were arranged in an alternating order to avoid local transfer biases.

Proteins were then wet-transferred to a PVDF membrane (Hybond-P, GE Healthcare Amersham, MU60103A) using the Mini Blot Module Set (ThermoFisher) in 1X NuPAGE Transfer Buffer (ThermoFisher) containing 10% methanol. Protein membranes were blocked in 5% skimmed milk TBST or 5% BSA TBST for 1 h at room temperature before incubation with primary antibodies overnight at 4°C. After 3–5 5-min washes with TBST, the membranes were incubated with species-specific secondary antibody conjugated to horseradish peroxidase (HRP) in TBST-milk for 1 h at room temperature. Then, membranes

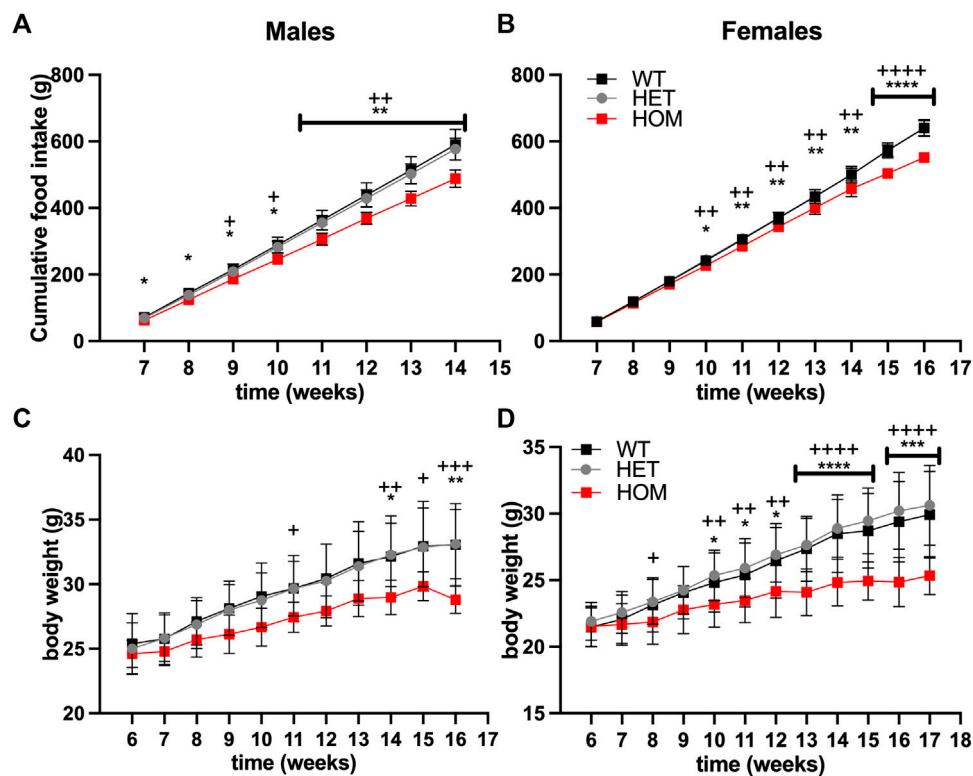


FIGURE 3

Food Intake and bodyweight are reduced in *Wars2^{V117L/V117L}* mice. Cumulative food intake in (A) males ($n = 4-10$) and (B) females ($n = 8-9$). N represents one cage of two mice of the same genotype. Bodyweight in the same cohort of (C) males ($n = 8-20$) and (D) females ($n = 12-18$) where N represents each mouse. Significance at specific time points was calculated with 1-way ANOVA with multiple comparisons. Significance symbols for WT \times HET: *, HET \times HOM: +.

were washed 5×5 min in TBST. The chemiluminescent reaction was carried out using the Pierce ECL Plus Western Blotting Substrate (ThermoFisher) and membranes imaged by exposure to CL-Xposure Film (ThermoFisher). Protein bands were quantified using ImageJ and normalised to the respective house-keeping gene. Primary antibodies used in this study: UCP1 at 1:1,000 dilution (Abcam, ab23841), α -tubulin at 1:10,000 (Cell Signalling, 2144).

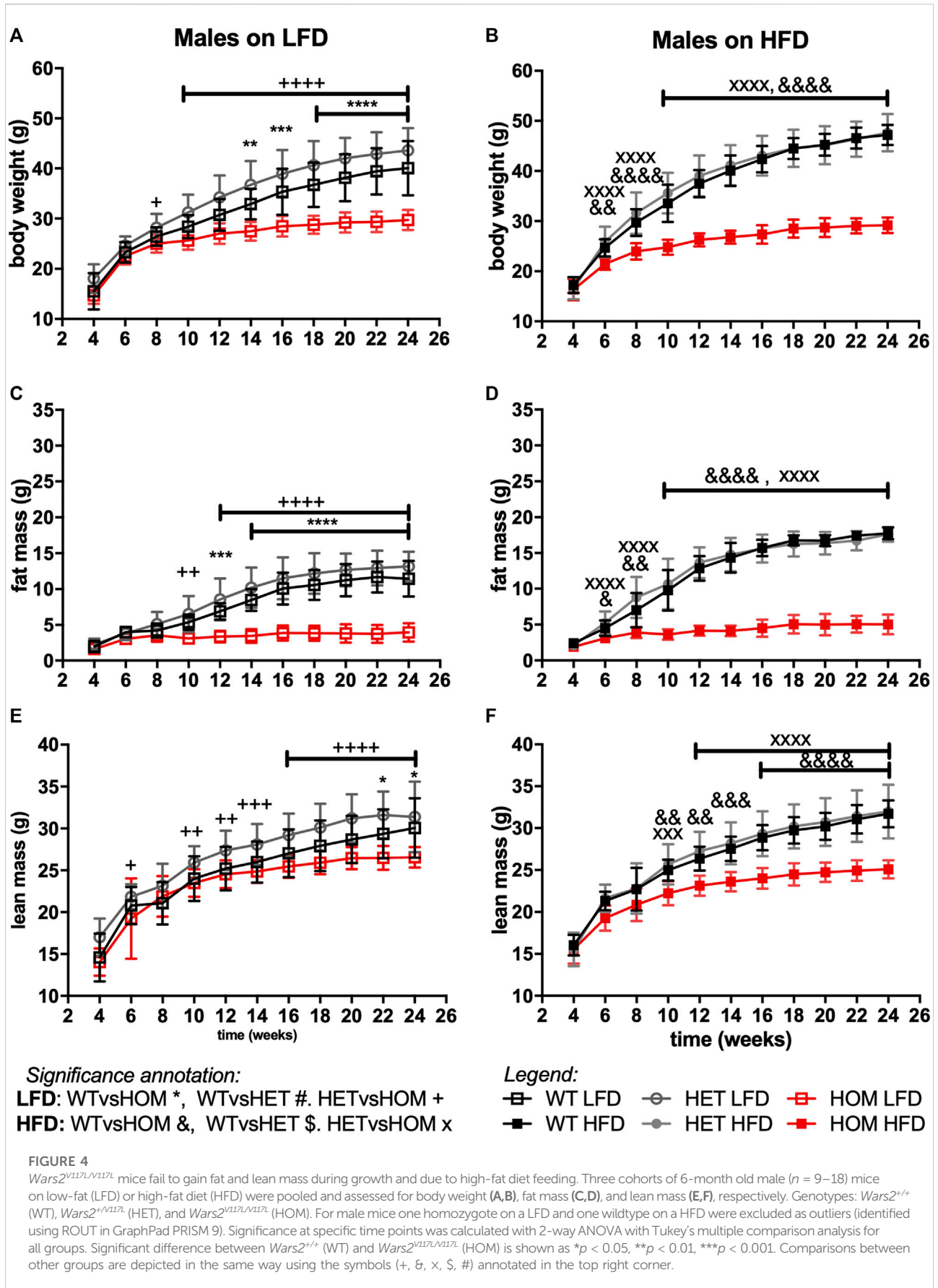
Mitochondrial DNA copy number assay

Mitochondrial content in adipose tissue was assessed by ratio of mitochondrial DNA (mtDNA) to genomic DNA (gDNA) as assessed using qRT-PCR. Total DNA, which contains both gDNA and mtDNA, was extracted from adipose tissue (experiment 1) using the Dneasy Blood and Tissue Kit (Qiagen, # 69504). We amplified both the mouse genomic gene *Glyceraldehyde 3-phosphate dehydrogenase* (*Gapdh*) and mouse mitochondrial gene Mitochondrially encoded NADH: Ubiquinone oxidoreductase core subunit 1 (*mt-Nd1*) as

proxies for genomic and mitochondrial DNA, respectively. Quantitative PCR was performed with 10 ng DNA per reaction and $5 \mu\text{M}$ of each primer, using the Fast SYBR Green System on a ABIPRISM 7500 Fast Real-Time PCR Machine (Applied Biosystems). All samples were run in technical triplicates. Primers: *mt-Nd1-Fw* (CCCATTCGCGTTATTCTT), *mt-Nd1-Rv* (AAGTTGATCGTAACGGAAAGC), *Gapdh-Fw* (CAAGGAGTAAGAAACCTGGACC), *Gapdh-Rv* (CGA GTTGGGATAGGGCCTCT).

Biochemical assays

Plasma fibroblast growth factor-21 (FGF21) levels were measured in blood plasma using Quantikine ELISA Mouse/Rat FGF21 Immunoassay (Quantikine, # MF2100). Mouse growth/differentiation factor 15 (GDF15) was measured using an in-house microtitre plate-based two-site electrochemiluminescence immunoassay using the MesoScale Discovery assay platform (MSD, Rockville, Maryland, United States). GDF-15 antibodies and standards were from R&D Systems (DuoSet # DY6385 BioTechne: Abingdon, UK).



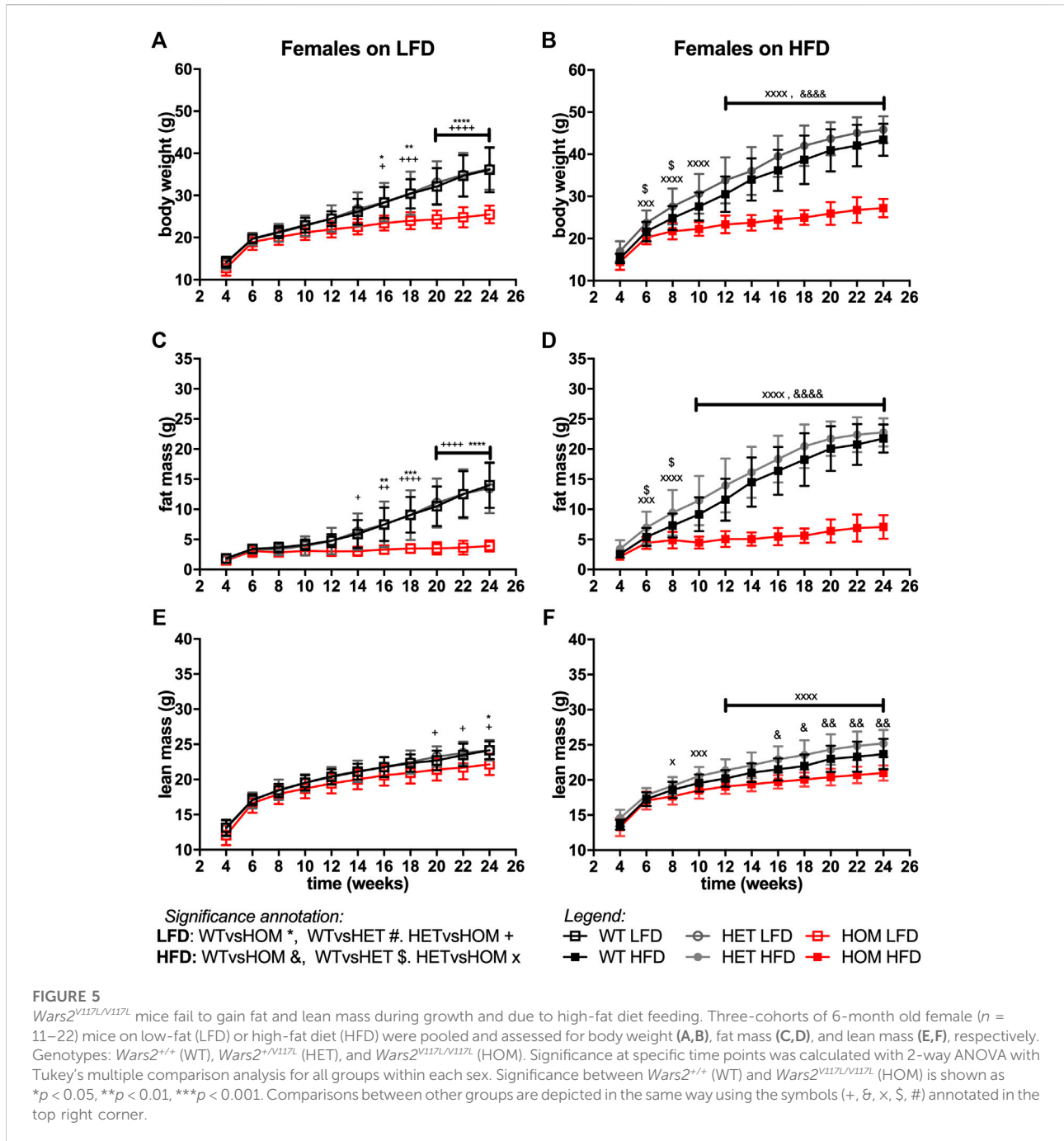


FIGURE 5
Wars2^{V117L/V117L} mice fail to gain fat and lean mass during growth and due to high-fat diet feeding. Three-cohorts of 6-month old female ($n = 11-22$) mice on low-fat (LFD) or high-fat diet (HFD) were pooled and assessed for body weight (A,B), fat mass (C,D), and lean mass (E,F), respectively. Genotypes: *Wars2^{+/+}* (WT), *Wars2^{+V117L}* (HET), and *Wars2^{V117L/V117L}* (HOM). Significance at specific time points was calculated with 2-way ANOVA with Tukey's multiple comparison analysis for all groups within each sex. Significance between *Wars2^{+/+}* (WT) and *Wars2^{V117L/V117L}* (HOM) is shown as * $p < 0.05$, ** $p < 0.01$, *** $p < 0.001$. Comparisons between other groups are depicted in the same way using the symbols (+, #, x, \$, #) annotated in the top right corner.

Statistical analysis

All statistical analyses were performed in Graph Pad Prism 9. Data outliers were identified using ROUT and omitted as indicated in each figure legend. Normality of distribution was evaluated using D'Agostino & Pearson normality test. Data was transformed where necessary in

order to normalise their distribution prior to statistical analysis and details of the statistical tests used are described in each figure legend. Area under the curve for bodyweight, fat and lean mass was calculated in PRISM with $Y = 0$ as a baseline. qPCR data was log-transformed and is shown as mean \pm SD for visualisation and statistical analysis.

Results

Browning is increased in both subcutaneous and visceral WAT depots of *Wars2*^{V117L/V117L} mice on chow diet

We set out to test whether browning effects previously observed in subcutaneous iWAT can also be observed in visceral gWAT, assessed by mRNA expression of a panel of browning and mitochondrial biogenesis gene markers in these mice at 4-months of age. In male iWAT of *Wars2*^{V117L/V117L} mice, as expected, we found increased expression of browning genes: *Cidea* increased by 0.61 ± 0.25 logFC ($p = 0.0343$), cytochrome c oxidase polypeptide 7A (*Cox7a*) by 0.60 ± 0.25 logFC ($p = 0.0414$) and *Dio2* by 0.93 ± 0.30 logFC ($p = 0.0133$) in (Figure 1A). Male gWAT showed 0.56 ± 0.13 logFC ($p = 0.0025$) and 0.53 ± 0.10 logFC ($p = 0.0006$) increase in mRNA levels of both *Cidea* and the master regulator of mitochondrial biogenesis peroxisome proliferator-activated receptor gamma coactivator 1- α (*Pgc1 α*) in *Wars2*^{V117L/V117L} mice (Figure 1B). In female iWAT of *Wars2*^{V117L/V117L} mice, *Cidea*, *Cox7a*, *Pgc1 α* , and *Ppara* were increased by 0.49 ± 0.15 , 0.47 ± 0.15 , 0.50 ± 0.12 and 0.33 ± 0.11 logFC, respectively ($p = 0.0122$, 0.0130 , 0.0026 , 0.0179 , respectively) (Supplementary Figure S1A). The expression of browning genes in female gWAT was highly variable and *Pgc1 α* was the only significantly upregulated gene 0.51 ± 0.17 logFC ($p = 0.0176$) in *Wars2*^{V117L/V117L} mice (Supplementary Figure S1B). We then assessed browning by immunoblotting for UCP1 protein in iWAT. In males, we found a significant increase ($p = 0.0437$) and a similar nonsignificant trend in females (Figures 1C,D; Supplementary Figures S1C,D). We next assessed mitochondrial mass as another marker of browning. Using a qPCR assay targeting both mtDNA and gDNA genes, we observed a significant increase of 0.43 ± 0.08 logFC and 0.23 ± 0.08 logFC in mtDNA: gDNA in male *Wars2*^{V117L/V117L} iWAT ($p = 0.0002$) and gWAT ($p = 0.0264$), respectively in *Wars2*^{V117L/V117L} mice (Figure 1E). No genotype driven difference was seen in female mice (Supplementary Figure S1E). In agreement with previous findings, BAT showed the reverse effect with reduced mitochondrial DNA content in both sexes (Supplementary Figure S2E), reduced expression of browning marker gene expression in both sexes in *Wars2*^{V117L/V117L} mice (Supplementary Figures S2A,B) and lower UCP1 expression in males and a trend for reduction in females (Supplementary Figures S2C,D). Together this is evidence of increased WAT browning, observed on multiple levels (mRNA, protein, mtDNA) in both iWAT and gWAT depots in *Wars2*^{V117L/V117L} mice with the specific effects differing between sexes and iWAT generally showing higher differences in fold change.

Mitokines FGF21 and GDF15 are elevated in the *Wars2*^{V117L/V117L} mice on chow diet

12-month old *Wars2*^{V117L/V117L} mice were previously shown to have mitochondrial ETC complex deficiencies in multiple tissues and elevated plasma levels of the mitokine, FGF21 which may at least partially explain the WAT browning. We thus decided to measure circulating FGF21 and the appetite-suppressing mitokine GDF15 in free fed 4-month old mice (Patel et al., 2019). We observed an overall genotype effect ($p = 0.0485$) on FGF21 levels, with an 86% increase ($p = 0.0364$) in female *Wars2*^{V117L/V117L} mice and a non-significant trend for increase in males (Figure 2A). GDF15 was significantly increased in *Wars2*^{V117L/V117L} mice of both sexes, with an 112% increase ($p = 0.0014$) in males and 158% increase ($p = 0.0001$) in females (Figure 2B). We followed with a qPCR study of multiple tissues to show that *Fgf21* expression was elevated by 1.80 ± 0.13 mean difference of log₁₀-fold change (logFC) \pm (SE) ($p = 0.0012$), 0.38 ± 0.11 logFC ($p = 0.0055$), 0.47 ± 0.16 logFC ($p = 0.0157$), 0.41 ± 0.18 logFC ($p = 0.0447$) in the heart, BAT, muscle and kidney of *Wars2*^{V117L/V117L} mice respectively (Figure 2C). *Gdf15* was elevated by 0.66 ± 0.09 of logFC ($p < 0.0001$) and 0.84 ± 0.12 logFC ($p < 0.0001$) in the heart and BAT, respectively (Figure 2D). We also tested for changes in *Atf4* levels, one of the upstream regulators of *Gdf15* and *Fgf21*, but found no difference in any of the tissues (Supplementary Figure S3).

Food intake is reduced in *Wars2*^{V117L/V117L} mice on a chow diet

We hypothesised that the elevated GDF15 levels may be contributing to reduced food intake in *Wars2*^{V117L/V117L} mice. To test an effect on food intake, we set up an independent cohort of pair-housed mice on regular RM3 chow diet. Male *Wars2*^{V117L/V117L} mice showed reduced cumulative food intake compared to wild-type mice already from the first timepoint at 7 weeks of age ($p = 0.045$) (Figures 3A,B). Female *Wars2*^{V117L/V117L} mice showed significantly lower food intake from 10 weeks onwards ($p = 0.0148$). At 14 weeks of age, the male and female cumulative food intake was 17% ($p = 0.0016$) and 8.4% lower than wild-type ($p = 0.0020$), respectively (Figures 3A,B). This is thus likely to have contributed to the lower bodyweight seen in these mice (Figures 3C,D).

Homozygous *Wars2*^{V117L/V117L} mice fail to gain fat mass due to growth and high-fat diet

In data from a small cohort of 6-month old *Wars2*^{V117L/V117L} males we previously showed a trend towards increased ratio of gWAT:iWAT mass (Agnew

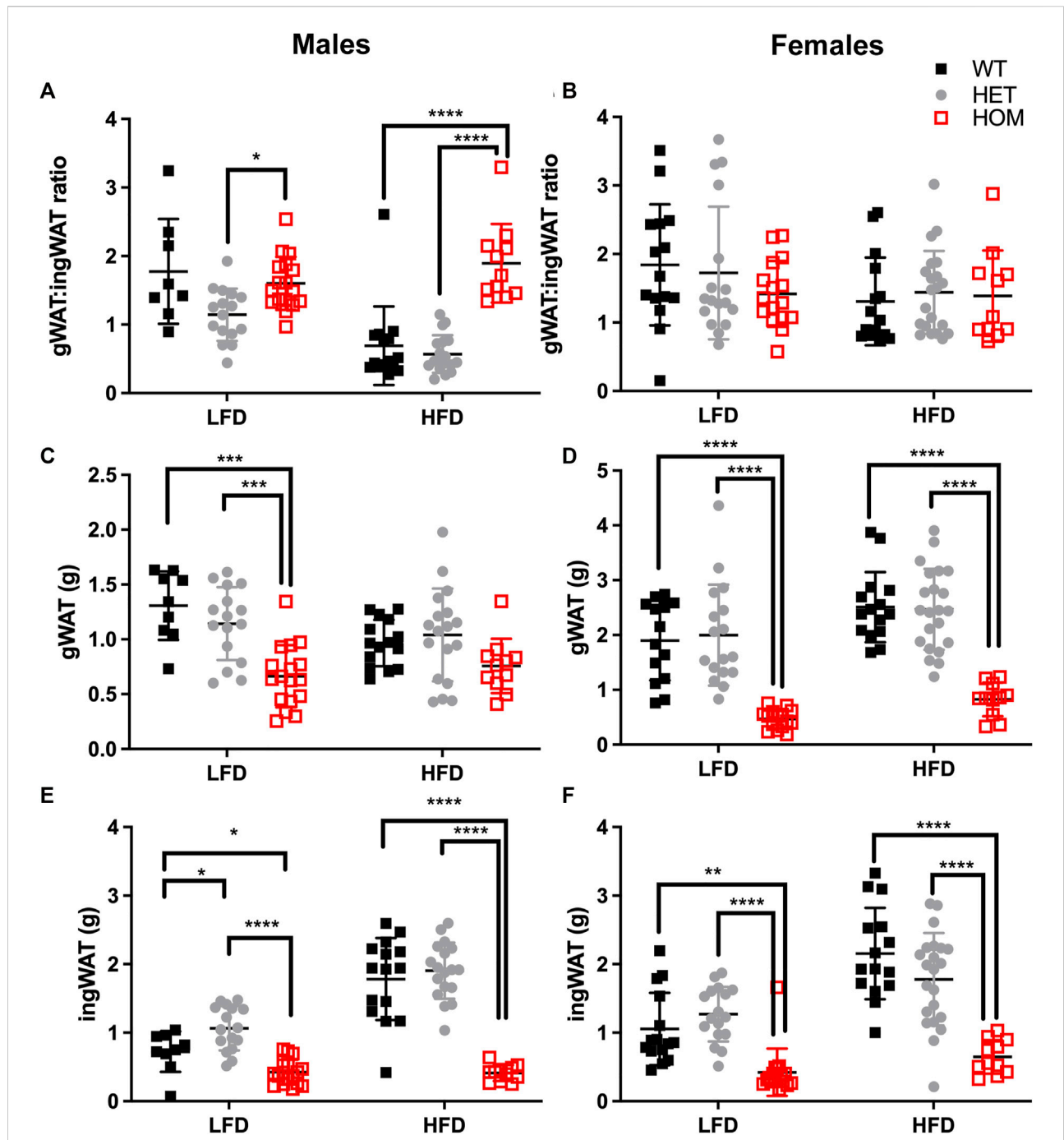


FIGURE 6
 Gonadal to inguinal WAT (gWAT: iWAT) ratio is elevated in *Wars2^{V117L/V117L}* males on a HFD. gWAT:iWAT ratio was calculated for 6-month old male ($n = 9-18$) and female ($n = 11-22$) mice either on low fat (LFD) and high-fat diets (HFD) (A,B). The individual gWAT (C,D) and iWAT (E,F) weights are shown below. To fit a normal distribution, male and female gWAT:iWAT ratio data and male iWAT data were transformed by $Y = \text{Log}_2(Y)$. The gWAT male and female data were normally distributed (D'Agostino & Pearson normality test) and the iWAT female data showed some deviation from normality ($p = 0.0476$). Significance was tested using 2-way ANOVA with Tukey's multiple comparison test between genotype for each diet. Significant differences in multiple comparisons of WT, HET and HOM on each diet are depicted as * $p < 0.05$, ** $p < 0.01$, *** $p < 0.001$.

et al., 2018). To investigate whether an altered diet could reveal a fat distribution phenotype or whether it would alleviate the failure to gain fat mass found in these mice, *Wars2^{V117L/V117L}*, *Wars2^{+V117L}* and *Wars2^{+/+}* mice were placed on HFD and matched LFD. As expected, HFD increased body weight and fat mass in wild-type *Wars2^{+/+}* (week 24, males: $p < 0.0001$, $p < 0.0001$; females: $p < 0.0001$, $p < 0.0001$, respectively) and heterozygous *Wars2^{+V117L}* mice (week 24, males: $p = 0.0363$, $p < 0.0001$, females: $p < 0.0001$, $p < 0.0001$, respectively). However, no significant effect of HFD on body weight was observed in *Wars2^{V117L/V117L}* mice of either sex (Figures 4A,B, 5A,B). On LFD, significant bodyweight differences between wild-type and *Wars2^{V117L/V117L}* were observed and persisted from 14 ($p = 0.0126$) and 16 weeks of age ($p = 0.0176$) for males and females, respectively. On a HFD, significance was reached earlier, at 6 ($p = 0.0016$) and 12 ($p < 0.0001$) weeks of age, respectively. Similar effects were observed between wildtype and homozygous mice for fat mass, which was significant from 6 to 12 weeks (male) and 10 and 16 weeks (female), 6 weeks earlier on HFD than on LFD, respectively (Figures 4C,D, 5C,D). Significant differences were also observed in the lean mass of *Wars2^{V117L/V117L}* mice, but these were of a smaller magnitude (Figures 4E,F, 5E,F). When analysed over the time course using area under curve, these differences were maintained (Supplementary Table S1). In summary, most of the weight differences in *Wars2^{V117L/V117L}* mice were due to the reduction in fat mass and administering a high-fat diet exacerbated these differences.

For all three measures, heterozygous *Wars2^{+V117L}* mice also showed significant differences to *Wars2^{V117L/V117L}* mice at an earlier age than for wild type mice (Figures 4A–F, 5A–F). A significant increase in bodyweight ($p = 0.0476$, $p = 0.0416$) and fat mass ($p = 0.0418$, $p = 0.0430$) of *Wars2^{+V117L}* females on HFD was observed compared to wild-type mice at 6 and 8 weeks of age respectively, but this change did not persist in later timepoints. In line with this, 12-month-old heterozygous female knockout *Wars2^{+/-}* mice did not show any differences in body weight or composition on either diet (Supplementary Figure S6). In summary, we did not observe any reproducible differences between the heterozygous *Wars2^{+V117L}* or *Wars2^{+/-}* mice and the wild-type mice.

Wars2^{V117L/V117L} mice show reduction in the weights of multiple fat depots and a HFD and male specific elevation in gWAT:iWAT ratio

Since the majority of the weight differences in the *Wars2^{V117L/V117L}* mice could be explained by fat mass, we next evaluated differences in fat distribution by weighing fat depots from 24 week old mice, and we considered the ratio of gWAT:

iWAT mass (Figure 6; Supplementary Figures S4, S5). Indeed, almost all fat depots weighed less in *Wars2^{V117L/V117L}* compared to wild-type or heterozygous mice. The only exceptions were male HFD gWAT, female HFD perirenal BAT and female LFD perirenal WAT which did not differ from *Wars2^{+/+}* or *Wars2^{+V117L}*. The lack of weight change in male *Wars2^{V117L/V117L}* gWAT on HFD together with the 1.372 ± 0.1755 g lower iWAT weight ($p < 0.0001$) resulted in an increased gWAT:iWAT ratio ($p < 0.0001$), indicating higher visceral to subcutaneous fat ratio (Figures 6A,C,E). Interestingly, no such trend was replicated in females where both iWAT and gWAT depot weights were reduced, by 1.508 ± 0.2398 g ($p < 0.001$) and 1.684 ± 0.2521 g ($p < 0.001$), respectively (Figures 6B,D,F). No significant differences were observed between the heterozygous and wild-type mice for any of the fat depots apart for male iWAT on a LFD ($p < 0.05$). Similarly, fat depots of 12-month-old female heterozygous *Wars2^{+/-}* mice in a separate cohort, did not show any significant differences (Supplementary Figure S7). This demonstrates that *Wars2^{V117L/V117L}* mice have much lower fat mass which is unequally shared by different fat depots and results in male and HFD-specific increase in gWAT:iWAT ratio.

Discussion

We assessed fat depot differences in browning and showed that the magnitude of browning effects is greater in iWAT than in gWAT of chow-fed 4-month-old *Wars2^{V117L/V117L}* mice. This agrees with previous research which showed that gWAT has low browning marker expression and a very low browning capacity compared to iWAT (de Jong et al., 2015; Zuriaga et al., 2017). Our findings suggest that the adipose phenotypes in *Wars2^{V117L/V117L}* mice are driven systemically, secondary to a severe mitochondrial dysfunction in the heart, BAT and muscle. Firstly, we confirmed the upregulation of FGF21, an established inducer of WAT browning (Fisher et al., 2012; Agnew et al., 2018). It is possible that other inducers of browning such as catecholamines could also be involved but were not measured in this study (Frontini et al., 2013). Secondly, we showed higher plasma GDF15 in these mice which may contribute to the observed lower food intake that thus contributed to the reduced bodyweight and fat mass, as shown in other models of mitochondrial disease (Chung et al., 2017).

We have shown that *Wars2^{V117L/V117L}* mice fail to gain fat mass also when challenged with a HFD, accompanied by a male and HFD-specific upregulation of gWAT:iWAT ratio. This was likely driven by the lower mass of iWAT and the relatively unchanged visceral gWAT on HFD. In general, all other male visceral depots showed a reduction of fat mass in male *Wars2^{V117L/V117L}* mice. It would be interesting to extend these observations using other methods, such as small animal X-ray computed tomography (CT) system, that could accurately verify

the effect on overall fat distribution over time (Sasser et al., 2012). This male-specific effect is in line with sexual dimorphism which is an established feature of fat distribution (Pulit et al., 2017). In fact, the *TBX15-WARS2* locus also contains an independent male-specific WHRadjBMI-association signal (Shungin et al., 2015). Further study will be required to explain the diet specificity. However, HFD was previously shown to induce browning and it could thus potentiate the depot-specific differences observed in chow-fed animals and thus contribute to HFD-specific fat mass loss seen in WAT and not gWAT (García-Ruiz et al., 2015).

It is important to note that all mice in this study were housed at “room temperature” (21°C ± 2°C) and not at thermoneutral temperature for small rodents (29°C–30°C). Housing mice at room temperature leads to a mild cold stress and permits browning of WAT (e.g., McKie et al., 2019; Raun et al., 2020), while not directly influencing fat mass (Small et al., 2018). Since we did not house mice at thermoneutrality it is not possible to discern whether the browning gene expression effect, or indeed the fat depot differences we detected in *Wars2*^{V117L/V117L} mice would be maintained under thermoneutral conditions, and this would be an interesting experiment to be tested in further investigations outside the scope of this study. Nevertheless, mice harbouring the *Wars2*^{V117L/V117L} mutation have greater mRNA expression of browning markers in WAT, greater UCP1 protein and greater mitochondrial mass than their wildtype littermates, demonstrating browning of the WAT in these mice. Whether this is a direct effect of the *Wars2*^{V117L/V117L} mutation or an interaction between the genotype and ambient temperature cannot be discerned by our current study.

Is it possible that a similar mechanism relating mitochondrial failure in the heart and other tissues together with WAT browning might drive the WHR signal in humans? Indeed, rare variants in genes of the mitochondrial genomes and in another member of the *ARS2* family, *DARS2*, have all been associated with WHR (Justice et al., 2019). Furthermore, in the Common Metabolic Diseases Knowledge Portal, the *TBX15-WARS2* locus is associated with cardiovascular traits such as stroke severity and peripheral vascular disease in people with type 2 diabetes (cmdgenkp.org, 2021a), whilst variants in the *WARS2* gene are linked to diastolic blood pressure (cmdgenkp.org, 2021b). This suggests that a systemic mechanism could explain the WHR GWAS association in humans.

In conclusion, we have shown that a hypomorphic mutation in the *Wars2* gene causes a severe failure to gain body mass and results in changes to fat distribution in male mice on a HFD. We also reveal differences in browning propensity of different WAT depots and elevation of circulating FGF21 and GDF15 which likely partly explain some of these phenotypes. These data

support a potential functional role for *WARS2* in the WHRadjBMI *TBX15-WARS2* locus, which could be further investigated in human studies where *WARS2* expression varies by genotype.

Data availability statement

The original contributions presented in the study are included in the article/Supplementary Material, further inquiries can be directed to the corresponding authors.

Ethics statement

Mice were kept and studied in accordance with UK Home Office legislation and local ethical guidelines issued by the Medical Research Council (Responsibility in the Use of Animals for Medical Research, July 1993; Home Office license 30/3146 and 30/3070). Procedures were reviewed and approved by the MRC Harwell Animal Welfare and Ethical Review Board (AWERB).

Author contributions

MM, RC, and RD designed and supervised the experiments, analysed data, prepared figures, and wrote the manuscript with input from all authors. MM carried out the molecular studies and body composition measurements. Food intake analysis was carried out by LB, MM, and LV. Cohorts were managed by LB and LV. Fat depot weight measurements were performed by MY, RD, and MM. LZ assisted with molecular studies. KB and PB carried out the GDF15 ELISAs.

Funding

This work was funded by the Medical Research Council (MC_U142661184). MM was funded by an MRC Doctoral Training studentship. GDF15 assays were conducted at the MRC MDU Mouse Biochemistry Laboratory (MC_UU_00014/5).

Acknowledgments

We thank Emily File in the MLC for excellent technical assistance. A preprint version of this manuscript was previously uploaded to bioRxiv (Mušo et al., 2022).

Conflict of interest

The authors declare that the research was conducted in the absence of any commercial or financial relationships that could be construed as a potential conflict of interest.

Publisher's note

All claims expressed in this article are solely those of the authors and do not necessarily represent those of their affiliated

organizations, or those of the publisher, the editors and the reviewers. Any product that may be evaluated in this article, or claim that may be made by its manufacturer, is not guaranteed or endorsed by the publisher.

Supplementary material

The Supplementary Material for this article can be found online at: <https://www.frontiersin.org/articles/10.3389/fphys.2022.953199/full#supplementary-material>

References

- Agnew, T., Goldsworthy, M., Aguilar, C., Morgan, A., Simon, M., Hilton, H., et al. (2018). A *Wars2* mutant mouse model displays OXPHOS deficiencies and activation of tissue-specific stress response pathways. *Cell Rep.* 25 (12), 3315–3328. e6. doi:10.1016/j.celrep.2018.11.080
- Canoy, D. (2008). Distribution of body fat and risk of coronary heart disease in men and women. *Curr. Opin. Cardiol.* 23 (6), 591–598. doi:10.1097/HCO.0b013e328313133a
- Chung, H. K., Ryu, D., Kim, K. S., Chang, J. Y., Kim, Y. K., Yi, H. S., et al. (2017). Growth differentiation factor 15 is a myomitokine governing systemic energy homeostasis. *J. Cell Biol.* 216 (1), 149–165. doi:10.1083/jcb.201607110
- Civelek, M., Wu, Y., Pan, C., Raulerson, C. K., Ko, A., He, A., et al. (2017). Genetic regulation of adipose gene expression and cardio-metabolic traits. *Am. J. Hum. Genet.* 100 (3), 428–443. doi:10.1016/j.ajhg.2017.01.027
- cmdgenkp.org (2021a) Common metabolic diseases Knowledge portal. TBX15-WARS2 locus Available at: <https://hugeamp.org/region.html?chr=1&end=119712077&phenotype=HEIGHT&start=118698196> (Accessed June 27, 2021).
- cmdgenkp.org (2021b). Common metabolic diseases Knowledge portal. WARS2. Available at: <https://hugeamp.org/gene.html?gene=WARS2> (Accessed June 27, 2021).
- de Jong, J. M. A., Larsson, O., Cannon, B., and Nedergaard, J. (2015). A stringent validation of mouse adipose tissue identity markers. *Am. J. Physiol. Endocrinol. Metab.* 308 (12), E1085–E1105. doi:10.1152/ajpendo.00023.2015
- Emdin, C. A., Khera, A. V., Natarajan, P., Klarin, D., Zekavat, S. M., Hsiao, A. J., et al. (2017). Genetic association of waist-to-hip ratio with cardiometabolic traits, type 2 diabetes, and coronary heart disease. *JAMA - J. Am. Med. Assoc.* 317 (6), 626–634. doi:10.1001/jama.2016.21042
- Fisher, F. F., Kleiner, S., Douris, N., Fox, E. C., Mepani, R. J., Verdeguer, F., et al. (2012). FGF21 regulates PGC-1 α and browning of white adipose tissues in adaptive thermogenesis. *Genes Dev.* 26 (3), 271–281. doi:10.1101/gad.177857.111
- Frontini, A., Vitali, A., Perugini, J., Murano, I., Romiti, C., Ricquier, D., et al. (2013). White-to-Brown transdifferentiation of omental adipocytes in patients affected by pheochromocytoma. *Biochim. Biophys. Acta* 1831 (5), 950–959. doi:10.1016/j.bbali.2013.02.005
- García-Ruiz, E., Reynes, B., Diaz-Rua, R., CErEsi, E., Oliver, P., and Palou, A. (2015). The intake of high-fat diets induces the acquisition of Brown adipocyte gene expression features in white adipose tissue. *Int. J. Obes.* 39 (11), 1619–1629. doi:10.1038/ijo.2015.112
- Gray, S. L., Nora, E. D., Grosse, J., Manieri, M., Stoeger, T., Medina-Gomez, G., et al. (2006). Leptin deficiency unmasks the deleterious effects of impaired peroxisome proliferator-activated receptor gamma function (P465L PPARgamma) in mice. *Diabetes* 55, 2669–2677. doi:10.2337/db06-0389
- GTEx-Consortium (2013). The genotype-tissue expression (GTEx) project. *Nat. Genet.* 45 (6), 580–585. doi:10.1038/ng.2653
- Heid, I. M., Jackson, A. U., Randall, J. C., Winkler, T. W., Qi, L., Steinthorsdottir, V., et al. (2010). Meta-analysis identifies 13 new loci associated with waist-hip ratio and reveals sexual dimorphism in the genetic basis of fat distribution. *Nat. Genet.* 42 (11), 949–960. doi:10.1038/ng.685
- Justice, A. E., Karaderi, T., Highland, H. M., Young, K. L., Graff, M., Lu, Y., et al. (2019). Protein-coding variants implicate novel genes related to lipid homeostasis contributing to body-fat distribution. *Nat. Genet.* 18, 452–469. doi:10.1038/s41588-018-0334-2
- Mason, C., Craig, C. L., and Katzmarzyk, P. T. (2008). Influence of central and extremity circumferences on all-cause mortality in men and women. *Obes. (Silver Spring)* 16 (12), 2690–2695. doi:10.1038/oby.2008.438
- Maurano, M. T., Humbert, R., Rynes, E., Thurman, R. E., Haugen, E., Wang, H., et al. (2012). Systematic localization of common disease-associated variation in regulatory DNA. *Science* 337 (6099), 1190–1195. doi:10.1126/science.1222794
- McKie, G. L., Medak, K. D., Knuth, C. M., Shamshoum, H., Townsend, L. K., Peppler, W. T., et al. (2019). Housing temperature affects the acute and chronic metabolic adaptations to exercise in mice. *J. Physiol.* 597 (17), 4581–4600. doi:10.1113/JP278221
- Mullican, S. E., Lin-Schmidt, X., Chin, C. N., Chavez, J. A., Furman, J. L., Armstrong, A. A., et al. (2017). GFRAL is the receptor for GDF15 and the ligand promotes weight loss in mice and nonhuman primates. *Nat. Med.* 23 (10), 1150–1157. doi:10.1038/nm.4392
- Mušo, M., Bentley, L., Vizor, L., Yon, M., Burling, K., Barker, P., et al. (2022). A *Wars2* mutant mouse shows a sex and diet specific change in fat distribution, reduced food intake and depot-specific upregulation of WAT browning. *bioRxiv*. doi:10.1101/2022.05.23.493147
- Myint, P. K., Kwok, C. S., Luben, R. N., Wareham, N. J., and Khaw, K. T. (2014). Body fat percentage, body mass index and waist-to-hip ratio as predictors of mortality and cardiovascular disease. *Heart* 100 (20), 1613–1619. doi:10.1136/heartjnl-2014-305816
- Patel, S., Alvarez-Guaita, A., Melvin, A., Rimmington, D., Dattilo, A., Miedzobrodzka, E. L., et al. (2019). GDF15 provides an endocrine signal of nutritional stress in mice and humans. *Cell Metab.* 29 (3), 707–718. e8. doi:10.1016/j.cmet.2018.12.016
- Peters, S. A. E., Bots, S. H., and Woodward, M. (2018). Sex differences in the association between measures of general and central adiposity and the risk of myocardial infarction: Results from the UK biobank. *J. Am. Heart Assoc.* 7 (5), e008507. doi:10.1161/JAHA.117.008507
- Potter, P. K., Bowl, M. R., Jeyarajan, P., Wisby, L., Bleasdale, A., Goldsworthy, M. E., et al. (2016). Novel gene function revealed by mouse mutagenesis screens for models of age-related disease. *Nat. Commun.* 7, 12444. doi:10.1038/ncomms12444
- Pravenec, M., Zidek, V., Landa, V., Mlejnek, P., Silhavy, J., SiMakovaM., et al. (2017). Mutant *Wars2* gene in spontaneously hypertensive rats impairs Brown adipose tissue function and predisposes to visceral obesity. *Physiol. Res.* 66 (6), 917–924. doi:10.33549/physiolres.933811
- Pulit, S. L., Karaderi, T., and Lindgren, C. M. (2017). Sexual dimorphisms in genetic loci linked to body fat distribution. *Biosci. Rep.* 37 (1), BSR20160184. doi:10.1042/BSR20160184
- Pulit, S. L., Stoneman, C., Morris, A. P., Wood, A. R., Glastonbury, C. A., Tyrrell, J., et al. (2018). Meta-analysis of genome-wide association studies for body fat distribution in 694,649 individuals of European ancestry. *Hum. Mol. Genet.* 28, 166–174. doi:10.1093/hmg/ddy327
- Raun, S. H., Henriquez-Olguin, C., Karavaeva, I., Ali, M., Moller, L. L. V., Kot, W., et al. (2020). Housing temperature influences exercise training adaptations in mice. *Nat. Commun.* 11 (1), 1560. doi:10.1038/s41467-020-15311-y
- Sasser, T. A., Chapman, S. E., Li, S., Hudson, C., Orton, S. P., Diener, J. M., et al. (2012). Segmentation and measurement of fat volumes in murine obesity models using X-ray computed tomography. *J. Vis. Exp.* 62, e3680. doi:10.3791/3680

- Shungin, D., Winkler, T. W., Croteau-Chonka, D. C., Ferreira, T., Locke, A. E., Magi, R., et al. (2015). New genetic loci link adipose and insulin biology to body fat distribution. *Nature* 518 (7538), 187–196. doi:10.1038/nature14132
- Small, L., Gong, H., Yassmin, C., Cooney, G. J., and Brandon, A. E. (2018). Thermoneutral housing does not influence fat mass or glucose homeostasis in C57BL/6 mice. *J. Endocrinol.* 239 (3), 313–324. doi:10.1530/JOE-18-0279
- Snijder, M. B., Dekker, J. M., Visser, M., Bouter, L. M., Stehouwer, C. D. A., Kostense, P. J., et al. (2003). Associations of hip and thigh circumferences independent of waist circumference with the incidence of type 2 diabetes: The hoorn study. *Am. J. Clin. Nutr.* 77 (5), 1192–1197. doi:10.1093/ajcn/77.5.1192
- Vazquez, G., Duval, S., Jacobs, D. R., and Silventoinen, K. (2007). Comparison of body mass index, waist circumference, and waist/hip ratio in predicting incident diabetes: A meta-analysis. *Epidemiol. Rev.* 29, 115–128. doi:10.1093/epirev/mxm008
- Wang, M., Sips, P., Khin, E., Rotival, M., Sun, X., Ahmed, R., et al. (2016). Wars2 is a determinant of angiogenesis. *Nat. Commun.* 7, 12061. doi:10.1038/ncomms12061
- Wang, Y., Rimm, E. B., Stampfer, M. J., Willett, W. C., and Hu, F. B. (2005). Comparison of abdominal adiposity and overall obesity in predicting risk of type 2 diabetes among men. *Am. J. Clin. Nutr.* 81 (3), 555–563. doi:10.1093/ajcn/81.3.555
- Zuriaga, M. A., Fuster, J. J., Gokce, N., and Walsh, K. (2017). Humans and mice display opposing patterns of “browning” gene expression in visceral and subcutaneous white adipose tissue depots. *Front. Cardiovasc. Med.* 4, 27. doi:10.3389/fcvm.2017.00027